Title: **Kynurenic acid, a key L-tryptophan-derived metabolite, protects the heart from an ischemic damage**

Einat Bigelman[1], Metsada Pasmanik-Chor[2], Bareket Dassa[3], Maxim Itkin[4], Sergey Malitsky[4], Orly Dorot[5], Edward Pichinuk[5], Smadar Levin-Zaidman[6], Nili Dezorella[6], Atan Gross[7], Anastasia Abashidze[5] Yuval Kleinberg[1], Gad Keren[1], Michal Entin-Meer[1*]

1- Laboratory of Cardiovascular Research, Tel Aviv Sourasky Medical Center, affiliated with the Sackler Faculty of Medicine, Tel-Aviv University, Tel-Aviv, Israel. This author takes responsibility for all aspects of the reliability and freedom from bias of the data presented and their discussed interpretation.

2- Bioinformatics Unit, Faculty of Life Sciences, Tel-Aviv University, Tel-Aviv, Israel. This author takes responsibility for all aspects of the reliability and freedom from bias of the data presented and their discussed interpretation.

3- Bioinformatics Unit, Department of Life Sciences Core Facilities, Weizmann Institute of Science, Rehovot, Israel. This author takes responsibility for all aspects of the reliability and freedom from bias of the data presented and their discussed interpretation.

4- Metabolic Profiling Unit, Life Sciences Core Facilities, Weizmann Institute of Science, Rehovot, Israel. This author takes responsibility for all aspects of the reliability and freedom from bias of the data presented and their discussed interpretation.

5- Bio-Imaging Core, Blavatnik Center for Drug Discovery, Tel-Aviv University, Tel-Aviv, Israel. This author takes responsibility for all aspects of the reliability and freedom from bias of the data presented and their discussed interpretation.

6- Electron microscopy unit, Weizmann Institute of Science, Rehovot, Israel. This author takes responsibility for all aspects of the reliability and freedom from bias of the data presented and their discussed interpretation.

7- Faculty of Biology, Department of Biological Regulation, Department of Life Sciences, Weizmann Institute of Science, Rehovot, Israel. This author takes responsibility for all aspects of the reliability and freedom from bias of the data presented and their discussed interpretation.

*Corresponding author: Michal Entin Meer, Cardiovascular Research laboratory, Tel-Aviv Sourasky medical Center, 6 Weizmann St, Tel-Aviv, Israel; 6423906. Tel:+972-3-6974205, Email:michale@tlvmc.gov.il.

Highlights

- The levels of the L- Tryptophan-derived metabolite, Kynurenic acid (KYNA), are significantly elevated in the heart and the plasma of animals induced with an acute kidney disease.
- KYNA rescues the viability of cardiac cells from an ischemic damage both *in vitro* and *in vivo*.
- KYNA can protect the structure & function of cardiac mitochondria in H9C2 cardiomyoblast cells upon exposure to anoxia.

Abstract:

Background: Renal injury induces major changes in plasma and cardiac metabolites. We sought to identify a key metabolite that may affect cardiac mitochondria following an acute kidney injury (AKI) that may be harnessed to protect the heart following an acute ischemic event.

Methods and Results: Metabolomics profiling of cardiac lysates and plasma samples derived from rats that underwent AKI 1 or 7 days earlier by 5/6 nephrectomy versus sham-operated controls was performed. We detected only 26 differential metabolites in both heart and plasma samples at the two selected time points, relative to sham. Out of which, kynurenic acid (kynurenate, KYNA) seemed most relevant. Interestingly, KYNA given at 10 mM concentration significantly rescued the viability of H9C2 cardiac myoblast cells grown under anoxic conditions and largely improved their mitochondrial structure and function as determined by flow cytometry and cell staining with MitoTracker dyes. Moreover, KYNA diluted in the drinking water of animals induced with an acute myocardial infarction, highly enhanced their cardiac recovery according to echocardiography and histopathology.

Conclusion and translational aspect: KYNA may represent a key metabolite absorbed by the heart following AKI. This metabolite can enhance cardiac cell viability following an ischemic event in a mechanism that is mediated, at least in part, by the protection of the cardiac mitochondria. A short-term administration of KYNA may be highly beneficial in the treatment of the acute phase of kidney disease in order to attenuate progression to CRS and in ischemic cardiac conditions to reduce ischemic myocardial damage.

Key words: Kynurenic acid, cardiac protection, ischemic damage, anoxia, cardiac mitochondria

Funding: The work was supported by the TASMC-Weizmann collaborative grant (212843) and the Azrieli award foundation.

Conflict of interest: N/A

Graphical abstract:

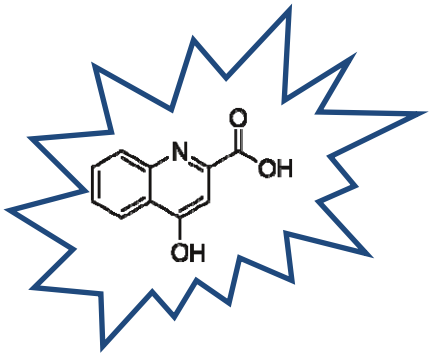

Induced cardiac & plasma concentration following AKI

KYNA

Binding

Enhanced intracellular $[Ca]^{2+}$- influx?

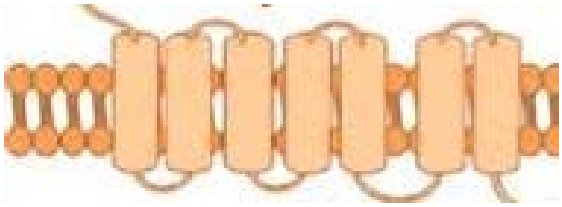

GPR35

(significantly accumulates on the cell surface upon anoxia)

GPR35 internalization

Reduced intracellular $[Ca]^{2+}$- influx?

Intracellular signaling

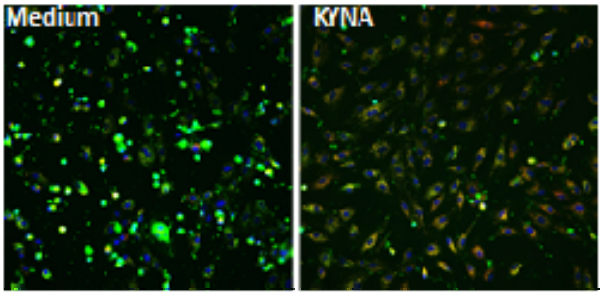

Salvaging cardiac mitochondria from an ischemic damage

Cardiomyocyte rescue from an ischemic insult

1. **Introduction:**

Concomitant cardiac and renal dysfunction, termed cardiorenal syndrome (CRS), has gained significant attention in the recent decade and is characterized into 5 types [1] . Type 3 and type 4 CRS, also known as renocardiac syndrome, are defined by acute or chronic kidney disease (AKI and CKD, respectively) and are associated with the development or progression of cardiac disease [2] . Kidney disease may directly or indirectly produce an acute cardiac event triggered by the inflammatory surge, oxidative stress and secretion of neurohormons [3-6]. Other known triggers for mainly-AKI mediated cardiac injuries and dysfunctions include AKI-related volume overload, metabolic acidosis and electrolyte disorders such as hyperkalemia and hypocalcemia [7]. Consequently, renal disease is considered a major risk for cardiovascular complications including acute myocardial infarction (AMI) and congestive heart failure. Recently, changes in cardiac mitochondrial dynamics and subsequent cardiac apoptosis have been suggested in a mouse renal ischemia-reperfusion (I/R) model. In this study, fragmented mitochondria in cardiomyocytes were observed after 30 min of bilateral renal I/R and reduction of fractional shortening was observed 72 h later [8]. Likewise, in our recent work, we have shown that sustained CKD induced in a rat model by 5/6 nephrectomy results in major cardiac pathology, including increased interstitial fibrosis, cardiomyocyte hypertrophy, induced expression of pro-apoptotic markers and massive spatial disarrangement of the cardiac muscle fibers. These changes were combined with significant mitochondrial damage as reflected by the swollen mitochondria in which the cristae density was reduced [9]. The processes were associated with an induced expression of the fission-related protein DRP1, suggesting that cardiac mitochondrial fragmentation takes place upon kidney injury [8, 9]. Interestingly, a recent study has demonstrated that AKI induces changes in 40% of the cardiac metabolites [10]. In this study, the authors documented that the post-AKI cardiac

metabolome was characterized by amino acid depletion, increased oxidative stress, and evidence of alternative energy production. In view of these data, in the current work, we wished to identify a key metabolite pathway whose expression is highly modified in both blood and cardiac lysates of Lewis rats induced with AKI in order to characterize a potential novel interventional tool for attenuating disease progression to CRS. Thorough metabolomics analysis revealed major changes in the L-tryptophan (TRP) metabolism pathway in general and a significant induction in kynurenic acid (kynurenate, KYNA), one of the major products of the TRP metabolism both in the blood and hearts of the experimental rats. Therefore we chose to focus in the current work on KYNA's effects on cardiac structure and function. Several lines of evidence suggest that G protein-coupled receptor 35 (GPR35) may serve as KYNA's receptor and that GPR35 can be activated and internalized into the cell by KYNA, which is found in the plasma in nano to micromolar concentrations [11]. Knock-out mice lacking GPR35 expression have been reported to have increased systemic blood pressure [12], but the mechanism is not known. In addition, high amounts of GPR35 were shown to be expressed in the wild-type mice hearts, and myocardial GPR35 gene expression was shown to be associated with human heart failure [13, 14].

In the current study, we analyzed the potential effects of KYNA on cardiac cell viability following exposure to ischemia using *in vitro* and *in vivo* models and assessed the possible involvement of the cardiac mitochondria in mediating the metabilte's effects. The data presented herein highlight the potential crucial importance of KYNA as a key metabolite that may offer cardiac protection under an ischemic event prevalent in patients suffering from renal dysfunction.

2. Materials & Methods:

2.1 Ethics statement

Animal studies were approved by The Animal Care and Use Committee of Tel Aviv Sourasky Medical-Center (6-1-18), which conforms to the policies of the American Heart Association and the Guide for the Care and Use of Laboratory Animals.

2.2 Animals

Male Lewis rats (250–350 gr)/ 12-week old female BALB/C mice were purchased from Envigo, Israel. Lewis rats were used for AKI studies and mice for AMI studies . All animals were kept under optimal conditions (food and water provided *ad libitum*) at room temperature in a temperature-controlled facility with 12 hrs. light/dark cycle. Prior to all surgical procedures, animals were anesthetized with a mixture of ketamine/xylazine (100/10 mg/kg, respectively) and anesthesia was confirmed by loss of pedal reflex (toe pinch). During experimental periods, animals were monitored 2–3 times per week for potential signs of suffering, mainly weight loss of more than 15% and significant changes in animals' behavior, mobility, or body posture. Should animals have met one of these criteria, euthanasia would have been warranted on the same day to prevent further suffering.

2.3 Rat model for AKI

Rats (4-5/group) underwent 5/6 nephrectomy for induction of AKI as previously established in our laboratory [9]. Briefly, 5/6 nephrectomy was performed in two consecutive surgeries: two-thirds of the left kidney was removed followed by removal of the right kidney a week later. Control animals underwent abdominal opening only (sham). The experiment was terminated one day or seven days following the second surgery.

2.4 Mice model for AMI

Twelve week-old BALB/C mice were randomized into two groups receiving tap water (control) or KYNA (250 mg/L) diluted in tap water (15 mice/arm) in accordance with previous reports [15]. Three

days later all animals were induced with AMI by permanent ligation of the left anterior descending artery (LAD) according to our established protocol [16]. To alleviate pain, subcutaneous injection of carprofen (5 mg/kg) was given during the surgery as well as once a day during the next three subsequent days. Five animals from the control group and six animals from the experimental group were excluded from the analysis due to one of the following reasons: normal cardiac function on day 1 (6 animals), animal's death prior to endpoint (4 animals) or weight loss of > 15% (1 animal). Consequently, the control and the experimental arms included 10 and 9 animals, respectively. The drinking water with or without KYNA was replaced twice a week until the end of the experiment on day 30 post surgery. Cardiac parameters on day one and day 30 post-infarction were obtained by echocardiography (Vevo 2100, VisualSonics, Toronto, Canada). Following the second echocardiography scan, mice were euthanized by CO_2 inhalation, and hearts were harvested and processed for histology.

2.5 Histological staining for collagen content

After embedding in paraffin, the blocks were sectioned into 5 μM slices and stained with Picro Sirius Red (PR, Direct Red 80, Sigma-Aldrich, St Louis, MO, USA) and hematoxylin to determine hypertrophy and the extent of left ventricular (LV) collagen scar .

2.6 Metabolites extraction and profiling

2.6.1. Tissue and plasma processing: The heart (LV) tissue was frozen in liquid nitrogen and then ground to powder using a mortar and pestle. The blood was withdrawn from the vena cava into blood collection tubes (BD Vacutainer). The tubes were centrifuged for two minutes at 4000 rpm, and the plasma samples were collected. Extraction and analysis of lipids and polar/semi-polar metabolites was performed as previously described [17-19] with some modifications. Plasma (100 μL) or ground lyophilized LV samples (20 mg) were extracted with 1 ml of a pre-cooled (−20˚C) homogenous

methanol:methyl-tert-butyl-ether (MTBE) 1:3 (v/v) mixture, containing following internal standards. The tubes were vortexed and then sonicated for 30 min in an ice-cold sonication bath (taken for a brief vortex every 10 min). Then, UPLC-grade water- methanol (3:1, v/v) solution (0.5 mL) was added to the tubes, followed by centrifugation. The upper organic phase was transferred into 2 mL Eppendorf tube. The polar phase was re-extracted as described above with 0.5 mL of MTBE. Both organic phases were combined and dried in speedvac and then stored at −80˚C until analysis. For analysis, the dried lipid extracts were re-suspended in 150 µL mobile phase B (see below) and centrifuged again at 13,000 rpm and 4˚C for 5 min. The lower polar phase used for polar and semi-polar metabolite analysis was stored at −80˚C until analysis.

2.6.2 LC-MS for lipidomics analysis: Lipid extracts were analyzed using a Waters ACQUITY UPLC system coupled to a Vion IMS QTof mass spectrometer (Waters Corp., MA, USA). Chromatographic conditions were as previously described .

2.6.3 Lipid identification and quantification: LC-MS data were analyzed and processed with UNIFI (Version 1.9.4, Waters Corp., MA, USA). The putative annotation of the lipid species was performed by comparison of accurate mass (below 3 ppm), fragmentation pattern, retention time (RT), and ion mobility (CCS) values to an in-house-generated lipid database. Peak intensities of the identified lipids were normalized to the internal standards and the amount of tissue used for analysis.

2.6.4 LC-MS for semi-polar metabolites analysis: Metabolic profiling of semi-polar phase was performed using Waters ACQUITY UPLC system coupled to a Vion IMS QTof mass spectrometer (Waters Corp., MA, USA). The LC separation was as previously described [18, 19].

2.6.5 Semi-polar compounds identification and data analysis: LC-MS data were analyzed and processed with UNIFI (Version 1.9.4, Waters Corp., MA, USA). The putative identification of the

different semi-polar species was performed by comparison accurate mass, fragmentation pattern, and ion mobility (CCS) values to in-house made semi-polar database when several compounds were identified vs. standards, when available.

2.6.6 LC-MS polar metabolite analysis and data analysis: Metabolic profiling of the polar phase was done as previously described [17, 19] with minor modifications described below. Briefly, the analysis was performed using an Aquity I class UPLC System combined with a mass spectrometer Q Exactive Plus (Orbitrap™, Thermo Fisher Scientific), which was operated in a negative ionization mode. Data processing was done using TraceFinder (Thermo Fisher Scientific) software when detected compounds were identified by retention time and fragments were verified using an in-house-generated mass spectra library.

2.6.7 Complete metabolomics analysis: AKI vs Sham: Metabolite intensities of both polar and semi-polar metabolites were normalized to cardiac mass (cardiac samples) or to sample volume (plasma samples) and analyzed using one-way ANOVA following a multiple correction step (FDR step-up). The comparison included control samples, time 24h and 1W samples for either heart, or plasma samples, separately. Metabolites were considered differential when detected in both groups, and had a linear |Fold-Change|>1.5, and FDR <0.05. For the specific analysis of the metabolites affiliated with the TRP catabolism pathway (Figure 1), the differences in raw intensities of these metabolites among the 3 groups (sham, 24h, 1w) were analyzed by one-way ANOVA followed by Tukey's post-hoc test (IBM SPSS Statistics 22 software). Significance was at $p<0.05$ (*$p<0.05$; $p<0.01$;***$p<0.001$).

2.7 H9C2 Cell viability assay

H9C2 myoblast cell line from rat myocardium (ATCC clone CRL-1446) was obtained as a generous gift from Dr. Gania Kessler-Icekson, Felsenstein Medical Research Center, Petach Tikva, Israel. The

cells were plated in 6 well plates (2.5 *10^5 cells/ well) in complete DMEM. A day later, the medium was replaced with serum-free DMEM with or without KYNA. Twenty-four hours later, the cells were exposed to anoxic (0% oxygen) or normoxic conditions for additional 48 hours. The cells were then collected, and their viability was tested using the annexin-PI apoptosis detection kit (MBL, USA) followed by flow cytometry analysis (BD Biosciences FACS Canto II).

2.8 Detection of cell surface GPR35

H9C2 were plated in 6 well plates (2.5 *10^5 cells/ well) in complete DMEM. A day later the medium was replaced with serum-free DMEM with or without 10 mM KYNA followed by exposure to normoxia/anoxia for another 48 hours. The cells were then trypsinized and stained with GPR35-FITC antibody, which recognizes the native form of the extracellular portion of the receptor (Biorbyt, England, clone orb399781) followed by flow cytometry analysis.

2.9 Cell staining and data analysis of mitochondrial morphology

H9C2 cells were plated in 96-well plates (10,000 cells/well). On the following day, the growth medium was replaced with serum-free DMEM, with or without KYNA (10 mM). Following 24 hours, the plates were exposed to normoxia/anoxia for 48 hours. The cells were stained using an automated High Content Imaging pipline (Freedom EVO 200 robot, Tecan Group Ltd., Männedorf, Switzerland) and imaged using the INCell 2200 automated microscope (GE Healthcare, ILL, USA) at X20 magnification (15 fields per well, 30 wells per condition). Following image acquisition, high-content image stacks were analyzed using the InCarta software (GE Healthcare) producing comparative fluorescence intensity measurements. Cell and nuclei morphology were determined by cytoplasmic and nuclear staining using Calcein Red-Orange (red, 0.30µM; #C34851, Thermo Fisher Scientific, MA, USA) and Hoechst (blue, 1.2µg/ml; #H1399, Thermo Fisher Scientific), respectively. In order to monitor the mitochondrial structure and function, the mitochondria were labeled with MitoTracker Green FM

(green, 0.25µg/ml; #M7514, Thermo Fisher Scientific) and MitoTracker Deep Red FM (far-red, 0.06µg/ml; #M22426, Thermo Fisher Scientific). To assess the mitochondrial oxidative damage, the same experimental groups (H9C2 cells which exposed to normoxia/anoxia with or without 10mM KYNA) were stained with MitoSox (red, 5µM; # M36008, Thermo Fisher Scientific, MA, USA), CalceinGreen (green, 0.83µM; # C3100MP, Thermo Fisher Scientific, MA, USA) and Hoechst. The results obtained from the InCarta software were further analyzed by utilizing a custom python script developed at the Blavatnik center for drug discovery at Tel-Aviv university, Israel. Following Z-score-based normalization, the quantification of Mito Activity was done by dividing the MitoTracker Deep Red intensity with MitoTracker Green intensity which was normalized with the cell intensity. Mito Fraction quantification was done by dividing the parameter of mitochondria organelles count of MitoTracker Deep Red with MitoTracker Green (Appendix Figure 2). The image in figures 3 was acquired by the INCell 2200 and exported to ImageJ software (http://rsb.info.nih.gov/ij/index.html).

2.10 Statistical analysis

SPSS (IBM® SPSS® Statistics; Version 22) was used for statistical analysis. All variables are expressed as means ± standard error of the mean (SEM). One-way ANOVA followed by Tukey's post-hoc test was used to compare the three groups (sham, AKI-24 h, AKI-1W). In the metabolomics analysis, ANOVA following a multiple correction step (FDR step-up) was performed using Partek Genomics Suite 7.0. In all tests, $p < 0.05$ was considered statistically significant.

Calculation: Kynurenic acid may harbor a significant role in protecting cardiomyocyte function in the setting of renal failure and help prevent progression to heart failure with either preserved or reduced ejection fraction. Morevover, this metabolite may have a role in mediating an enhanced recovery from an ischemic insult during myocardial infarction by maintaing the cardiomyocyte viability,

mitochondrial structure, and myocardial function and hence preventing progression to cardiorenal syndrome.

3. Results:

3.1 Metabolomics analysis

The metabolomics analysis identified a total of 468 metabolites in the heart, which include both polar and semi-polar metabolites (276 metabolites) as well as lipid metabolites (192 metabolites) (Appendix Table A.1). Out of which, 71 and 68 metabolites were differentially expressed in the heart at 24 h and one week time points, respectively, relative to sham (FC ≥ 1.5; one-way ANOVA, p≤ 0.05). Forty-one of these metabolites were differentially expressed at both time points relative to sham (listed as "Differential" in Appendix Table A.1). In the plasma, 440 metabolites which include both polar and semi-polar metabolites (245 metabolites) as well as lipid metabolites (195 metabolites) were identified (Appendix Table A.2). Out of which, 125 and 104 metabolites were differentially expressed at 24 h or 1 week, respectively, compared to sham (FC ≥ 1.5; one-way ANOVA, p≤ 0.05). Eighty-one of these metabolites were differentially expressed at both time points relative to sham (listed as "Differential" in Appendix Table A.2). A Venn diagram analysis between the 41 cardiac common metabolites and the 81 plasma common metabolites revealed 26 overlapping metabolites whose expression was up/down-regulated relative to sham (Appendix Figure B.1). Out of which, we chose to focus on kynurenate (kynurenic acid, KYNA)- a side-chain product of the TRP metabolism, which was already identified as a key metabolite highly secreted to the blood following AKI [20, 21] that may also be involved in cardiovascular physiology and pathology [20, 22, 23]. An ANOVA-analysis-based fold-change in the cardiac and plasma levels of the TRP pathway metabolites relative to sham is given in Figure 1. Cardiac KYNA levels were increased by 4.4-fold on day 1 and by 3.1-fold on day 7 following AKI

induction relative to sham animals. Likewise, in the plasma, KYNA levels were elevated by 22.6- fold and 17.8-fold on the same two time points, respectively ($p< 0.05$, Figure 1A). Concomitantly, TRP levels were reduced by 2.0-fold and 1.5-fold in the LV samples on day 1 and day 7, respectively ($p< 0.05$), and by 2.7 and 2.1-fold in their plasma samples; $p< 0.05$ (Figure 1B). Further analysis confirmed that kynurenine (KYN) -the major source key product of the TRP catabolism pathway, is also increased in the cardiac lysates as well as the plasma of the AKI animals at both time points (8.7 and 4.1-fold increase in the heart, 2.7 and 2.0-fold increase in the plasma on 1 day and day 7, respectively; $p< 0.05$, Figure 1C). A similar increase was measured in the levels of a downstream product of the kynurenine pathway Quinolinate that was detected in cardiac samples on day 1 and day 7 post AKI, but not in the sham animals (data not shown since the exact fold-change could not be determined). A marked increase of this metabolite was detected in the plasma samples on day one and day seven relative to sham; (9.0-fold and 4.4-fold, respectively $p< 0.01$, Figure 1D). As for the intermediate element in the KYNA pathway, 3-hydroxyanthranilate, this metabolite was detected only in the plasma at 24 hours' time point but neither in sham or seven days- plasma samples, nor in any cardiac sample (data not shown). Altogether, the results suggest that the TRP metabolism pathway in general and KYNA, in particular, may play an important role in the pathological changes that take place in the heart in the AKI setting (Figure 1E).

3.2 Cardiac cell protection

To assess the potential effects of KYNA on the viability of cardiac cells, we first tested the viability of H9C2 myoblast cells in the presence of increasing concentrations of KYNA by flow cytometry with annexin-FITC-PI, as demonstrated in Figure 2A. As expected, in the absence of KYNA, the viability of the cells was significantly reduced under anoxia (60.3 ± 3.7%) compared to normoxia (91.7 ± 0.4 %) ($p=0.01$). KYNA administered at a concentration of 5 mM or 10 mM resulted in a minor reduction in the viability of the cells grown under regular normoxic conditions (86.2 ± 0.7 % and 82.4 ± 1.3 %,

respectively; $p<0.05$). Surprisingly, however, preincubation with 5 mM or 10 mM KYNA significantly protected the cardiac cells from a proceeding anoxic damage (77.5 ± 1.9 % and 84.2 ± 1.0 % in the presence of 5 mM or 10 mM KYNA, respectively; $p< 0.05$). H9C2 cell viability was not affected at all when KYNA was administered at lower doses, neither under normoxia, nor under anoxia relative to control cells grown without KYNA. In view of the observed dramatic effect of KYNA when given at 10 mM concentration, we chose to use this dose in all our subsequent *in vitro* experiments. Representing captures of H9C2 cells grown with or without KYNA (10 mM) followed by exposure to normoxia or anoxia were taken under light microscopy. The captures support that KYNA induces cell salvage under anoxic conditions while slightly reducing cardiac cell viability under normoxic conditions (Figure 2B). Altogether, the data indicate that while KYNA given at a concentration of 10 mM slightly minimizes the viability of H9C2 under normoxic conditions, the metabolite salvages the cells from anoxia-related cell death.

3.3 GPR35 receptor internalization

The flow cytometry data presented herein (Figure 2C) demonstrate that anoxic conditions result in a significant increase in GPR35 surface expression relative to normoxia from 9.5% to 99.7% (P2+P3 gates), as previously suggested [14]. Exposure to KYNA leads to reduced GPR35 expression from the cell surface under normoxic conditions (1.0 %- P2 only) as well as under anoxic conditions (16.9 % versus 0.0% in the P3 gate which represents the high-GPR35 expressing cells), probably due to receptor internalization as previously reported [24]. The data suggest that the KYNA-GPR35 interaction may initialize an intracellular signaling cascade that results in H9C2 cell salvage upon exposure to anoxia.

3.4 Protection from anoxia-driven mitochondrial damage

H9C2 cells were grown under normoxia or anoxia, with or without prior exposure to KYNA. The cells were labled with Hoechst (nuclei), Calcein Red-Orange (cytoplasm), MitoTracker Green (FITC) FM (mitochondrial structure) and MitoTracker Deep Red FM (mitochondrial function). Principal Component Analysis (PCA) analysis confirmed that the combination of mitochondrial features capture 73% of the total variance in the data and displays a clear separation between the experimental conditions: normoxia-medium, normoxia-KYNA, anoxia-medium and anoxia- KYNA (Figure 3A). Representative captures for single stainings and merged staining for each experimental arm as well the statistical box plot analyses are given in Figure 3B & 3C. As expected, relative to standard normoxic conditions, exposure to anoxia significantly reduces the total cell count (1442.00 [1293.50-1596.25] vs 4937.50 [4827.5-5163.25]; p= 3.6*10-45), the mitochondrial fraction (0.419 [0.293-0.639] vs 0.845 [0.798-0.876]; p= $2.6*10^{-29}$) and the mitochondrial function (0.192 [0.081-0.287] vs 0.578 [0.529-0.601]; p= $2.3*10^{-20}$). In the presence of KYNA, the stainings confirm that this metabolite reduces the cell number under physiological conditions (3382.5 [3042.50-3529.50] vs 4937.6 [4827.50-5163.25]; p= $1.3*10^{-22}$, with or without KYNA respectively); however, KYNA slightly increases the cell number upon exposure to anoxia (1670 [1584.00-1795.00] vs 1442 [1293.50-1596.25]; p=0.002). Interestingly, staining with the two MitoTracker dyes demonstrated that KYNA improves the mitochondrial structure (MitoTracker Green: 0.879 [0.841-0.904] vs 0.845 [0.798-0.876]; p= $6.2*10^{-11}$) and function (MitoTracker Deep Red: 0.818 [0.772-0.864] vs 0.578 [0.529-0.601]; p= $3.65*10^{-22}$) under normoxia. A more pronounced mitochondrial protective effect was evident when KYNA was administerd prior to exposure to anoxia: MitoTracker Green: 0.575 [0.481-0.645] vs 0.419 [0.293-0.639]; p= $1.56*10^{-18}$ and MitoTracker Red: 0.505 [0.370-0.626] vs 0.192 [0.081-0.287]; p= $3.99*10^{-9}$. Altogether, the statistical analysis of the cell count, mitochondrial fraction and mitochondrial activity in the four groups confirms that administration of KYNA prior to exposure to anoxia results in an increased median cell number, increased mitochondrial fraction and increased mitochondrial activity relative to

cells exposed to anoxia only (one-way ANOVA, Figure 3C). We observed several significant parameters that confirm the rescue of H9C2 cells grown under anoxia (Appendix Figure B.2). The data thus indicate that KYNA may protect cardiac cell surviaval, at least in part, by ameliorating the anoxic-mediated mitochondrial damage.

3.5 Cardiac protection in a murine model for AMI

Based on the *in vitro* data pointing to cardiac protection upon O_2 restriction, we sought to assess the effects of KYNA provided in the drinking water in an *in vivo* model for AMI induced by a permanent LAD ligation. The echocardiography, presented in Figure 4A, shows that the median LV ejection fraction (EF) values in the vehicle-treated animals were only slightly and insignificantly reduced between day 1 and day 30 (41.7 % vs 34.6 %, p=0.6, non-parametric median test). Interestingly, the median EF value of the animals treated with KYNA was significantly higher on day 30 relative to day 1 (55.5 % vs 43.2 %; $p< 0.001$, non-parametric median test). In line with these results, the data presented in Figure 4B demonstrate that the cardiac mass values are slightly increased in untreated animals on day 30 relative to day 1 (78.0 mg vs 67.2 mg, p=0.04). On the other hand, no significant difference was observed in the KYNA- treated mice between day 30 and day 1 in the median values of the cardiac mass (72.0 mg vs 70.2 mg, p=1.0). The histological staining for collagen content further supports the beneficial effect of KYNA on the cardiac scar size and interstitial fibrosis, as shown in the representative captures (Figure 4C).

Altogether, the *in vivo* data strongly suggest that KYNA protects cardiac function following an ischemic event, compared to post-AMI animals which are not treated with this metabolite.

Discussion:

Previous reports suggest that the TRP catabolism products might hold a role in mediating cardiovascular physiology and pathology [25-27], in addition to the regulation of the cardiac immune system functions and inflammation [28, 29]. The data presented in the current manuscript suggest that the TRP metabolism pathway in general and kynurenic acid, in particular, may play a significant role in mediating cardiac protection following AKI. Interestingly, the data point that KYNA may harbor a double-edged sword effect. Under normoxic conditions, elevated plasma and cardiac levels of KYNA may induce modest mitochondrial swelling and dysfunction and mediate cardiomyocyte cell death. However, increased levels of this metabolite may confer protective effects in the setting of myocardial infarction as suggested by the *in vitro* analysis of H9C2 cells exposed to anoxia and the *in vivo* model for AMI.

TRP metabolic pathway is activated during inflammatory conditions such as viral invasion, bacterial lipopolysaccharide or interferon-γ stimulation [30, 31]. TRP metabolism is well-controlled under physiological conditions but altered as part of the activated immune response. Indeed, dysregulated TRP catabolism has been linked to various diseases including neurodegenerative disorders, multiple sclerosis, schizophrenia, depression, diabetes, cancer, inflammatory bowel disease [32-34] and to an increased risk for AMI in patients with suspected angina pectoris [35].

Emerging evidence suggests that the reduced plasma concentrations of TRP concomitantly to the induced concentration of its metabolites may serve as vital biomarkers in the monitoring of several heart diseases, including AMI, atherosclerosis, and endothelial dysfunction as well as their risk factors [25-27]. Indeed, alteration in TRP catabolites was monitored in atherosclerosis and an elevated expression of indoleamine-2,3-dioxygenase (IDO)-1/2, the first and rate-limiting enzyme catabolizing both D and L-tryptophan to KYN was observed in the macrophage-rich cores of human advanced atherosclerotic plaques [36]. Moreover, several reports suggest that the cytokine interferon-gamma, which is released during the cell-mediated immune responses that take place in coronary heart diseases,

induces IDO-1 activity [28, 29]. Likewise, the potential involvement of metabolites derived from TRP catabolism in general and of KYN/KYNA, in particular has been demonstrated in the sera of patients with coronary heart disease (CHD). One study has shown that a significant proportion of patients with CHD present with decreased plasma TRP concentration which coincided with increased KYN/TRP ratio and also with increased neopterin concentrations indicating an activated immune response [28]. In addition, abnormal KYN/KYNA was found to be highly associated with endothelial dysfunction, which accounts for a significant portion of all cardiovascular diseases [37].

An elevated expression of metabolites derived from TRP catabolism was also reported in the plasma of patients suffering from kidney injury. One report showed an increased expression of the TRP catabolites L-KYN and quinolinic acid in the serum of both rat and human with renal insufficiency [21] and another one pointed to KYNA elevation in the sera of CKD patients, mainly in those suffering from polycystic kidney disease [20]. Likewise, recent findings suggest that the plasma concentrations of TRP and its catabolites might serve as biomarkers for the monitoring of AMI [25]. Yet, according to our knowledge, this is the first report that shows a marked elevation in TRP catabolites in the sera following AKI, concomitantly to their reduced expression in cardiac sections.

The data presented herein point that the metabolite whose levels were increased with a clear significance in both the heart and the plasma samples of AKI-induced animals, relative to sham-operated controls, is KYNA. Interestingly, while KYNA somewhat decreased the cellular viability and the mitochondrial structure and function and induced oxidative damage under physiological conditions in line with other reports [38], the metabolite significantly increased the viability and improved the structure, function, and the resistance to oxidative stress of the mitochondria of H9C2 cells exposed to anoxia. Moreover, KYNA enhanced cardiac recovery from an ischemic AMI *in vivo*. In line with these data, several reports point that KYNA is an important endogenous antioxidant and that its protective effects in diverse toxic models may stem from its redox characteristics [39, 40] in addition to its agonist

activity on its putative receptor, the previously orphan G-protein coupled receptor 35. There is evidence that KYNA may modify heart function, yet it is debatable whether these effects are beneficial or detrimental. On the one hand, KYNA was reported to decrease respiratory parameters, mainly the respiratory control index of glutamate/malate respiring heart mitochondria, and thus lead to the development of cardiomyopathy symptoms [23, 38]. On the other hand, cardio-protective effects of KYNA have also been proposed. For instance, KYNA was proven successful in decreasing the heart rate of spontaneously hypertensive rats without affecting the mean arterial pressure and thus it is suggested that KYNA may offer therapeutic potential as opposed to most drugs used to decrease heart rate that have strong adverse inotropic or hypotensive effects [41]. Recent reports show that KYNA may exert anti-inflammatory effects through GPR35 internalization and activation which in turn inhibits the release of TNFα by macrophages under LPS-induced inflammatory conditions [42]. In the heart, the expression of GPR35 may correlate with heart failure. Indeed, GPR35 was identified among the top 12 genes whose expression correlates with the severity of heart failure and adenoviral overexpression of GPR35 was shown to cause hypertrophic-like morphology changes and reduced cellular viability of cardiomyocytes [13]. Interestingly, recent reports suggest that the plasma membrane expression of GPR35 in cardiomyocytes is significantly induced under hypoxia and that application of an alternative GPR35 ligand, KYNA or zaprinast, induces GPR35 internalization and subcellular accumulation in the myocytes [14, 43]. Interestingly, it has been suggested that an *in vivo* administration of a siRNA to GPR35 enhances cardiac function following an acute MI through reduction of reactive oxygen species activity and mitochondria-dependent apoptosis [43]. The data presented herein suggest that KYNA administration prior to the induction of an ischemic event, leads to GPR35 intracellular internalization concomitantly to reduced cell death. We thus assume that receptor internalization or downregulated expression may protect the cardiomyocytes from cell membrane GPR35-mediated cell death and LV dysfunction. Previous studies have demonstrated that the KYNA-

GPR35 interactions can inhibit N-type Ca^{2+} channels in sympathetic neurons [44] and reduce the plateau phase of ATP-induced calcium transients in astrocytes [45]. Therefore it is yet to be clarified whether the elevated levels of GPR35 upon exposure to hypoxia result in increased detrimental Ca^{2+}-influx into the injured cardiomyocytes and whether the KYNA-mediated GPR35 internalization reduces these pathological enhanced Ca^{2+} transients. Thus, in line with these reports and data from our *in vitro* and animal studies, several mechanisms can be proposed to explain the dual-effect of KYNA that can potentially be harnessed for medical puposes. KYNA was shown to have antioxidant effect, it has effect on calcium ion influx and efflux and importantly on membranous presentation of GPR35 receptor and mainly internalization of the receptor upon exposue to high levels of the metabolite.

Conclusions: The data presented herein shed light on the tryptophan catabolism product, KYNA, which may represent a key metabolite absorbed by the heart following AKI. The data highly suggest that KYNA can enhance cardiac cell viability following an ischemic event both *in vitro* and *in vivo* in a mechanism which is mediated, at least in part, by the protection of the cardiac mitochondria from oxidative stress. Further research is warranted in order to determine whether KYNA can be developed into a therapeutic drug or a supplemental agent to be utilized in the multimodality treatment of post-AMI patients and in patients who are at high risk for experiencing an ischemic event, while minimizing its toxicity to cardiomyocytes under physiological conditions.

Study limitation: The effect of KYNA in our study was performed on a limited number of rodents and in a model of LAD complete ligation and not in a reperfusion injury model. An *in vivo* dose response should be carried out in order to determine the lowest therapeutic dose following cardiac ischemia. In addition, the exact mechanism of action of the KYNA-GPR35 axis which leads to cardiac protection following ischemia is yet to be deciphered.

Figures:

Figure 1: AKI significantly affects the expression of various metabolites related to TRP catabolism. (A-D) Box plot graphs showing the change of relative intensity in AKI-1d (n=5) and AKI-1W (n=4) versus the mean intensity value of the sham group (n=5) per each metabolite. Significance was calculated by one-way ANOVA followed by Tukey's post-hoc test *- $p< 0.05$, **- $p<0.01$, ***- $p< 0.001$. X- Denotes mean values, horizontal lines stands for the median values. (E) Schematic illustration of the TRP catabolite pathway demonstrating increased (red), decreased (blue) or unchanged (white) expression in AKI heart (H) and plasma (P) sections at 24 hours versus sham.

Figure 2: KYNA salvages H9C2 cell viability upon exposure to ischemic conditions. (A) Dose response for H9C2 cell viability grown in the presence of KYNA followed by exposure to normoxic or anoxic conditions, as determined by flow cytometry. Each box represents values derived from three independent experiments. * $p<0.05$; **$p< 0.01$ (One-way ANOVA). X- Denotes mean values, horizontal lines stands for the median values (B) Representative captures, derived from three independent experiments, showing H9C2 viability in the presence of 10 mM KYNA under normoxia versus anoxia. (C) Reduced cell surface expression of GPR35 following exposure to KYNA, determind by flow cytometry (two independent experiments with two technical replicates).

Figure 3: KYNA rescues H9C2 cells from anoxia-driven cell death and mitochondrial disruption. (A) A PCA analysis demonstrating a clear separation between experimental conditions by the combination of mitochondrial features (24-30 wells per treatment). (B) Representative images of mitochondrial structure (MitoTracker Green FM) and function (MitoTracker Deep Red FM) as well as nuclei (Hoechst) and cytoplasm (Calcein-Red-Orange) staining. The merged column represents the merging of Hoechst and the two MitoTracker dyes. (C) Box plot graphs demonstrating median and sample scattering of the values (24-30 wells per treatment) affiliated cell count, mitochondrial fraction and mitochondrial activity after Z-score-based normalization (see mitochondria data analysis description in Materials & Methods section). The statistical analysis (One-way ANOVA) is given in the text.

Figure 4: KYNA enhances cardiac recovery following AMI. Female BALB/C mice were treated with KYNA (250 mg/Lit) diluted in their drinking water (n=9) versus regular tap water (n=10). Treatment commenced 3 days prior to LAD ligation. KYNA treatment resulted in an elevated LV EF (%) at the experimental animals on day 30 relative to day 1 ($p=0.05$, paired 2-tailed t-test) (A) as well as in preservation of the cardiac mass on day 30 relative to day 1 as opposed to the marked increase of the cardiac mass (mg) in the control animals on day 30 relative to day 1 ($p=0.04$, paired 2-tailed t-test) (B). KYNA also reduced the amount of the collagen scar tissue in the heart according to Picro Sirius Red staining (captures representing six cardiac sections per each experimental arm are given) (C).

A.1: List of all metabolites detected in cardiac lysates of the experimental animals (arbitrary units). N/A- not applicable= below detection**.** Metabolite intensities of both polar and semi-polar metabolites were normalized to cardiac mass (cardiac samples) or to sample volume (plasma samples) and analyzed using ANOVA following a multiple correction step (FDR step-up), using Partek Genomics Suite 7.0. Differential metabolites whose levels are significantly modified in both 24h and 7 day- time points relative to sham are listed in the right column.

A.2: List of all metabolites detected in plasma samples of the experimental animals (arbitrary units). N/A- not applicable= below detection**.** Metabolite intensities of both polar and semi-polar metabolites were normalized to cardiac mass (cardiac samples) or to sample volume (plasma samples) and analyzed using ANOVA following a multiple correction step (FDR step-up), using Partek Genomics Suite 7.0. . Differential metabolites whose levels are significantly modified in both 24h and 7 day- time points relative to sham are listed in the right column.

B.1: Venn diagram yielding 26 differentially-expressed cardiac and plasma metabolites at both time points: 1 day and 1 week relative to sham.

B.2: Parameters which exhibit the rescue of H9C2 cells grown under anoxia in box plots graphs. (A) Quantification of Mito Activity and Mito fraction as documented in Figure 5. (B) Box plots graph representation of MitoTracker Deep Red intensity, MitoTracker red intensity, and cell intensity. (C) Box plots graph re-presentation of mitochondria elongation and area (24-30 replicates per arm).

Acknowledgments: Electron microscopy studies were conducted at the Irving and Cherna Moskowitz Center for Nano and Bio-Nano Imaging at the Weizmann Institute of Science.

References

[1] Ronco C, Di Lullo L. Cardiorenal syndrome. Heart failure clinics. 10 (2014) 251-280. 10.1016/j.hfc.2013.12.003.

[2] Di Lullo L, Bellasi A, Barbera V, Russo D, Russo L, Di Iorio B, Cozolino M, Ronco C. Pathophysiology of the cardio-renal syndromes types 1-5: An uptodate. Indian Heart J. 69 (2017) 255-265. 10.1016/j.ihj.2017.01.005.

[3] Yap SC, Lee HT. Acute kidney injury and extrarenal organ dysfunction: new concepts and experimental evidence. Anesthesiology. 116 (2012) 1139-1148. 10.1097/ALN.0b013e31824f951b.

[4] Prabhu SD. Cytokine-induced modulation of cardiac function. Circ Res. 95 (2004) 1140-1153. 10.1161/01.RES.0000150734.79804.92.

[5] Kaesler N, Babler A, Floege J, Kramann R. Cardiac Remodeling in Chronic Kidney Disease. Toxins (Basel). 12 (2020) 161. 10.3390/toxins12030161.

[6] Di Lullo L, House A, Gorini A, Santoboni A, Russo D, Ronco C. Chronic kidney disease and cardiovascular complications. Heart Fail Rev. 20 (2015) 259-272. 10.1590/1806-9282.66.S1.3.

[7] Kingma JG, Jr., Vincent C, Rouleau JR, Kingma I. Influence of acute renal failure on coronary vasoregulation in dogs. J Am Soc of Nephrol. 17 (2006) 1316-1324. 10.1681/ASN.2005101084.

[8] Sumida M, Doi K, Ogasawara E, Yamashita T, Hamasaki Y, Kariya T, Takimoto E, Yahagi N, Nagaku M, Noiri E. Regulation of Mitochondrial Dynamics by Dynamin-Related Protein-1 in Acute Cardiorenal Syndrome. J Am Soc of Nephrol. 26 (2015) 2378-2387. 10.1681/ASN.2014080750.

[9] Bigelman E, Cohen L, Aharon-Hananel G, Levy R, Rozenbaum Z, Saada A, Keren G, Entin-Meer M. Pathological presentation of cardiac mitochondria in a rat model for chronic kidney disease. PLoS One. 13(2018) e0198196. 10.1371/journal.pone.0198196.

[10] Fox BM, Gil HW, Kirkbride-Romeo L, Bagchi RA, Wennersten SA, Haefner KR, Skrypnyk NI, Brown CN, Soranno DE, Gist KM, Griffin BR, Jovanovich A, Reisz JA, Wither MJ, D'Alessandro A, Edelstein CL, Clendenen N, McKinsey TA, Altmann C, Faubel S. Metabolomics assessment reveals oxidative stress and altered energy production in the heart after ischemic acute kidney injury in mice. Kidney Int. 95 (2019) 590-610. 10.1016/j.kint.2018.10.020.

[11] Forrest CM, Mackay GM, Oxford L, Stoy N, Stone TW, Darlington LG. Kynurenine pathway metabolism in patients with osteoporosis after 2 years of drug treatment. Clin Exp Pharmacol Physiol . 33 (2006) 1078-1087. 10.1016/j.kint.2018.10.020.

[12] Divorty N, Milligan G, Graham D, Nicklin SA. The Orphan Receptor GPR35 Contributes to Angiotensin II-Induced Hypertension and Cardiac Dysfunction in Mice. Am J Hypertens. 31 (2018) 1049-1058. 10.1093/ajh/hpy073.

[13] Min KD, Asakura M, Liao Y, Nakamaru K, Okazaki H, Takahashi T, Fujimoto K, Ito S, Takahashi A, Asanuma H, Yamazaki S, Minamino T, Sanada S, Seguchi O, Nakano A, Ando Y, Otsuka T, Furukawa H, Isomura T, Takashima S, Mochizuki N, Kitakaze M. Identification of genes related to heart failure using global gene expression profiling of human failing myocardium. Biochem Biophys Res Commun. 393(2010) 55-60. 10.1016/j.bbrc.2010.01.076.

[14] Ronkainen VP, Tuomainen T, Huusko J, Laidinen S, Malinen M, Palvimo JJ, Ylä-Herttuala S, Vuolteenaho O, Tavi P. Hypoxia-inducible factor 1-induced G protein-coupled receptor 35 expression is an early marker of progressive cardiac remodelling. Cardiovasc Res. 101(2014) 69-77. 10.1093/cvr/cvt226.

[15] Turski WA, Malaczewska J, Marciniak S, Bednarski J, Turski MP, Jablonski M, Siwicki AK. On the toxicity of kynurenic acid in vivo and in vitro. Pharmacol Rep. 66 (2014) 1127-1133. 10.1016/j.pharep.2014.07.013.

[16] Entin-Meer M, Cohen L, Hertzberg-Bigelman E, Levy R, Ben-Shoshan J, Keren G. TRPV2 knockout mice demonstrate an improved cardiac performance following myocardial infarction due to attenuated activity of peri-infarct macrophages. PLoS One. 12 (2017) e0177132. 10.1371/journal.pone.0177132.

[17] Itkin M, Rogachev I, Alkan N, Rosenberg T, Malitsky S, Masini L, Meir S, Iijima Y, Aoki K, de Vos R, Prusky D, Burdman S, Beekwilder J, Aharoni A. GLYCOALKALOID METABOLISM1 is required for steroidal alkaloid glycosylation and prevention of phytotoxicity in tomato. Plant Cell. 23 (2011) 4507-4525. 10.1105/tpc.111.088732.

[18] Malitsky S, Ziv C, Rosenwasser S, Zheng S, Schatz D, Porat Z, Ben-Dor S, Aharoni A, Vardi A. Viral infection of the marine alga Emiliania huxleyi triggers lipidome remodeling and induces the production of highly saturated triacylglycerol. New Phytol. 210 (2016) 88-96. 10.1111/nph.13852.

[19] Gnainsky Y, Zfanya N, Elgart M, Omri E, Brandis A, Mehlman T, Itkin M, Malitsky A, Adamski K, Soen Y. Systemic Regulation of Host Energy and Oogenesis by Microbiome-Derived Mitochondrial Coenzymes. Cell Rep. 34 (2021) 108583. 10.1016/j.celrep.2020.108583.

[20] Grams ME, Tin A, Rebholz CM, Shafi T, Kottgen A, Perrone RD, Sarnak MJ, Inker LA, Levey AS, Coresh J. Metabolomic Alterations Associated with Cause of CKD. Clin J Am Soc Nephrol. 12 (2017) 1787-1794. 10.2215/CJN.02560317.

[21] Saito K, Fujigaki S, Heyes MP, Shibata K, Takemura M, Fujii H, Wada H, Noma A, **S**eishima M. Mechanism of increases in L-kynurenine and quinolinic acid in renal insufficiency. Am J Physiol Renal Physiol. 2000 279 (2000) F565-572. 10.1152/ajprenal.

[22] Badzynska B, Zakrocka I, Turski WA, Olszynski KH, Sadowski J, Kompanowska-Jezierska E. Kynurenic acid selectively reduces heart rate in spontaneously hypertensive rats. Naunyn-Schmiedeberg's archives of pharmacology. 393(2020) 673-679. 10.1007/s00210-019-01771-7.

[23] Baran H, Staniek K, Bertignol-Sporr M, Attam M, Kronsteiner C, Kepplinger B. Effects of Various Kynurenine Metabolites on Respiratory Parameters of Rat Brain, Liver and Heart Mitochondria. Int J Tryptophan Res. 9 (2016) 17-29. 10.4137/IJTR.S37973.

[24] Wang J, Simonavicius N, Wu X, Swaminath G, Reagan J, Tian H, Ling L. Kynurenic acid as a ligand for orphan G protein-coupled receptor GPR35. J Biol Chem. 281(2006) 22021-22028. 10.1074/jbc.M603503200.

[25] Tong Q, Song J, Yang G, Fan L, Xiong W, Fang J. Simultaneous determination of tryptophan, kynurenine, kynurenic acid, xanthurenic acid and 5-hydroxytryptamine in human plasma by LC-MS/MS and its application to acute myocardial infarction monitoring. Biomed Chromatogr. 32 (2018). 10.1002/bmc.4156.

[26] Santisukwongchote K, Amornlertwatana Y, Sastraruji T, Jaikang C. Possible Use of Blood Tryptophan Metabolites as Biomarkers for Coronary Heart Disease in Sudden Unexpected Death. Metabolites. 10 (2019) 6. 10.3390/metabo10010006.

[27] Song P, Ramprasath T, Wang H, Zou MH. Abnormal kynurenine pathway of tryptophan catabolism in cardiovascular diseases. Cell Mol Life Sci. 74 (2017) 2899-2916. 10.1007/s00018-017-2504-2.

[28] Wirleitner B, Rudzite V, Neurauter G, Murr C, Kalnins U, Erglis A, Fuchs D. Immune activation and degradation of tryptophan in coronary heart disease. Eur J Clin Invest. 33 (2003) 550-554. 10.1046/j.1365-2362.2003.01186.x.

[29] Wang Q, Liu D, Song P, Zou MH. Tryptophan-kynurenine pathway is dysregulated in inflammation, and immune activation. Front Biosci (Landmark Ed). 20 (2015) 1116-1143. 10.2741/4363.

[30] Mellor AL, Munn DH. IDO expression by dendritic cells: tolerance and tryptophan catabolism. Nat Rev Immunol. (2004) 762-774. 10.1038/nri1457.

[31] Taylor MW, Feng GS. Relationship between interferon-gamma, indoleamine 2,3-dioxygenase, and tryptophan catabolism. FASEB J. (1995):2516-2522. 10.1096/fasebj.5.14.1752366.

[32] Lovelace MD, Varney B, Sundaram G, Lennon MJ, Lim CK, Jacobs K, Guillemin GJ, Brew BJ. Recent evidence for an expanded role of the kynurenine pathway of tryptophan metabolism in neurological diseases. Neuropharmacology. 112 (2017):373-388. 10.1016/j.neuropharm.2016.03.024.

[33] Colpo GD, Venna VR, McCullough LD, Teixeira AL. Systematic Review on the Involvement of the Kynurenine Pathway in Stroke: Pre-clinical and Clinical Evidence. Front Neurol. 10 (2019) 778. 10.3389/fneur.2019.00778.

[34] Chen Y, Guillemin GJ. Kynurenine pathway metabolites in humans: disease and healthy States. Int J Tryptophan Res. 2 (2009) 1-19. 10.4137/ijtr.s2097.

[35] Pedersen ER, Tuseth N, Eussen SJ, Ueland PM, Strand E, Svingen GF, Midttun Ø, Meyer K, Mellgren G, Ulvik A, Nordrehaug JE, Nilsen DW, Nygård O. Associations of plasma kynurenines with risk of acute myocardial infarction in patients with stable angina pectoris. Arterioscler Thromb Vasc Biol. 35 (2015) 455-462. 10.1161/ATVBAHA.114.304674.

[36] Niinisalo P, Oksala N, Levula M, Pelto-Huikko M, Jarvinen O, Salenius JP, Kytömäki L, Soini JT, Kähönen M, Laaksonen R, Hurme M, Lehtimäki T. Activation of indoleamine 2,3-dioxygenase-induced tryptophan degradation in advanced atherosclerotic plaques: Tampere vascular study. Ann Med. 42(2010) 55-563. 10.3109/07853890903321559.

[37] Wang Q, Zhang M, Ding Y, Wang Q, Zhang W, Song P, eZou MH. Activation of NAD(P)H oxidase by tryptophan-derived 3-hydroxykynurenine accelerates endothelial apoptosis and dysfunction in vivo. Circ Res. 114 (2014) 480-492. 10.1161/CIRCRESAHA.114.302113.

[38] Baran H, Staniek K, Kepplinger B, Gille L, Stolze K, Nohl H. Kynurenic acid influences the respiratory parameters of rat heart mitochondria. Pharmacology. 62 (2001) 119-123. 10.1159/000056082.

[39] Lugo-Huitron R, Blanco-Ayala T, Ugalde-Muniz P, Carrillo-Mora P, Pedraza-Chaverri J, Silva-Adaya D, Maldonado PD, Torres I, Pinzón E, Ortiz-Islas E, López T, García, E, Pineda B, Torres-Ramos M, Santamaría A, Pérez-De La Cruz V. On the antioxidant properties of kynurenic acid: free radical scavenging activity and inhibition of oxidative stress. Neurotoxicol Teratol. 33 (2011) 538-547. 10.1016/j.ntt.2011.07.002.

[40] Hardeland R, Zsizsik BK, Poeggeler B, Fuhrberg B, Holst S, Coto-Montes A. Indole-3-pyruvic and -propionic acids, kynurenic acid, and related metabolites as luminophores and free-radical scavengers. Adv Exp Med Biol. 467 (1999) 389-395. 10.1007/978-1-4615-4709-9_49.

[41] Badzynska B, Zakrocka I, Turski WA, Olszynski KH, Sadowski J, Kompanowska-Jezierska E. Kynurenic acid selectively reduces heart rate in spontaneously hypertensive rats. Naunyn Schmiedebergs Arch Pharmacol. 393 (2020) 673-679. 10.1007/s00210-019-01771-7.

[42] Wang J, Simonavicius N, Wu X, Swaminath G, Reagan J, Tian H, Ling L. Kynurenic acid as a ligand for orphan G protein-coupled receptor GPR35. J Biol Chem. 281(2006) 22021-22028. 10.1074/jbc.M603503200.

[43] Chen K, He L, Li Y, Li X, Qiu C, Pei H, Yang D. Inhibition of GPR35 Preserves Mitochondrial Function After Myocardial Infarction by Targeting Calpain 1/2. J Cardiovasc Pharmacol. 75 (2020):556-563. 10.1097/FJC.0000000000000819.

[44] Guo J, Williams DJ, Puhl HL, 3rd, Ikeda SR. Inhibition of N-type calcium channels by activation of GPR35, an orphan receptor, heterologously expressed in rat sympathetic neurons. J Pharmacol Exp Ther. 324 (2008) 342-351. 10.1124/jpet.107.127266.

[45] Berlinguer-Palmini R, Masi A, Narducci R, Cavone L, Maratea D, Cozzi A, Sili M, Moroni F, Mannaioni G. GPR35 activation reduces Ca2+ transients and contributes to the kynurenic acid-dependent reduction of synaptic activity at CA3-CA1 synapses. PLoS One. 8(2013) e82180. 10.1371/journal.pone.0082180.

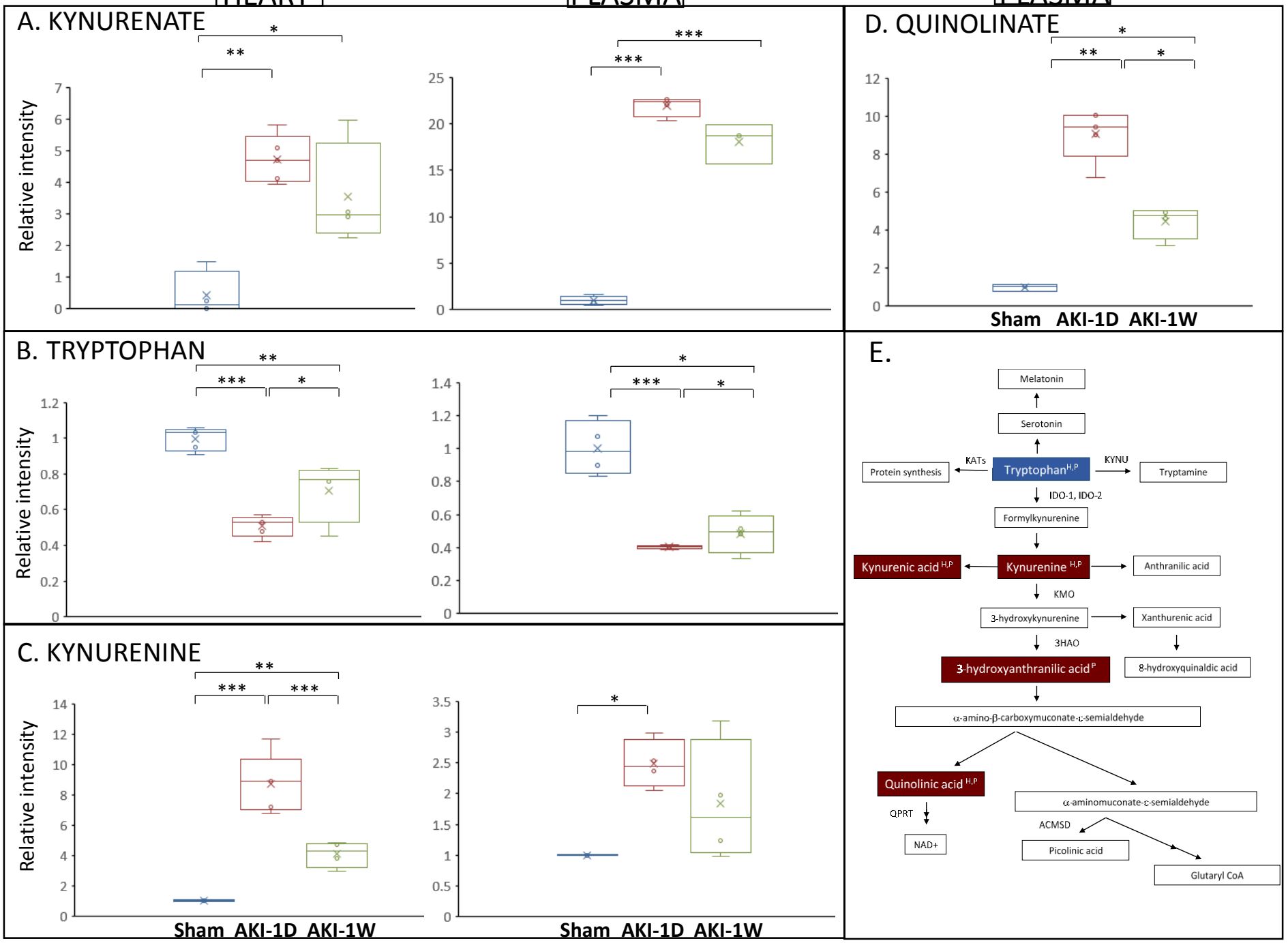
HEART
PLASMA
PLASMA
A. KYNURENATE
Relative intensity
B. TRYPTOPHAN
Relative intensity
C. KYNURENINE
Relative intensity
Sham AKI-1D AKI-1W
Sham AKI-1D AKI-1W
D. QUINOLINATE
Sham AKI-1D AKI-1W
E.
Melatonin
Serotonin
Protein synthesis
KATs
Tryptophan H,P
KYNU
Tryptamine
IDO-1, IDO-2
Formylkynurenine
Kynurenic acid H,P
Kynurenine H,P
Anthranilic acid
KMO
3-hydroxykynurenine
Xanthurenic acid
3HAO
3-hydroxyanthranilic acid P
8-hydroxyquinaldic acid
α-amino-β-carboxymuconate-ε-semialdehyde
Quinolinic acid H,P
α-aminomuconate-ε-semialdehyde
QPRT
NAD+
ACMSD
Picolinic acid
Glutaryl CoA

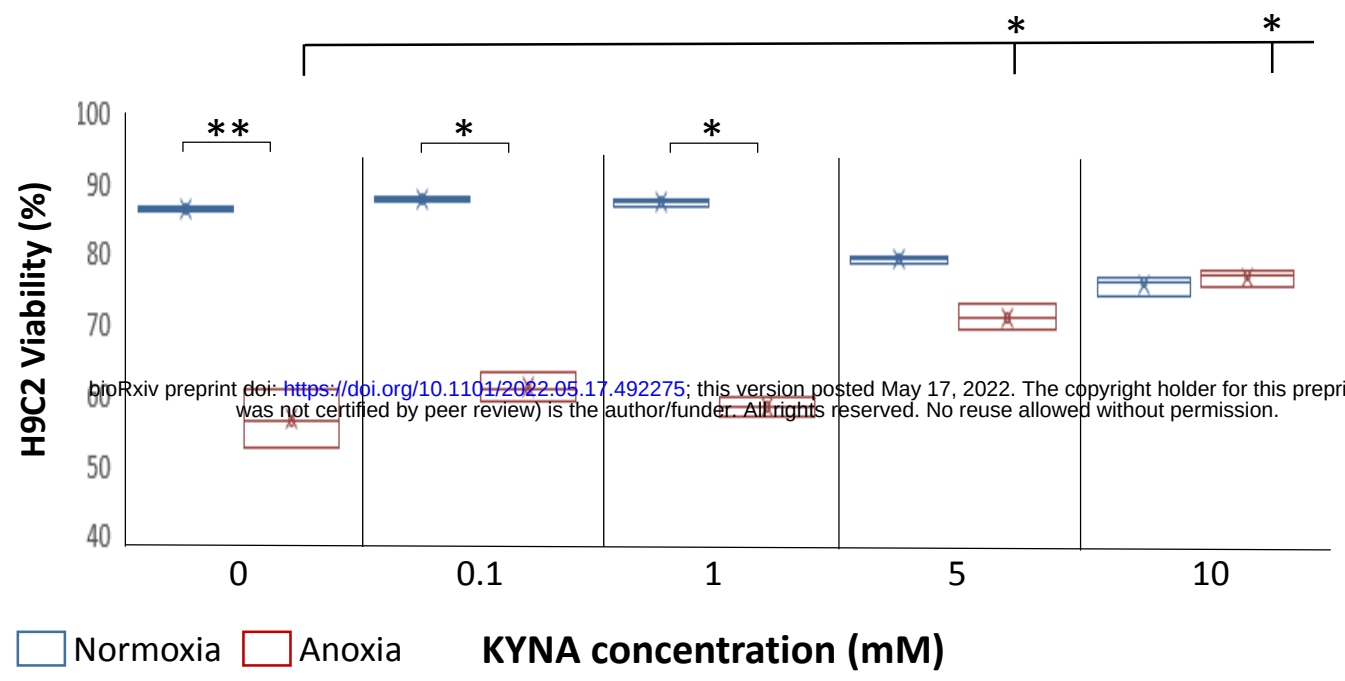

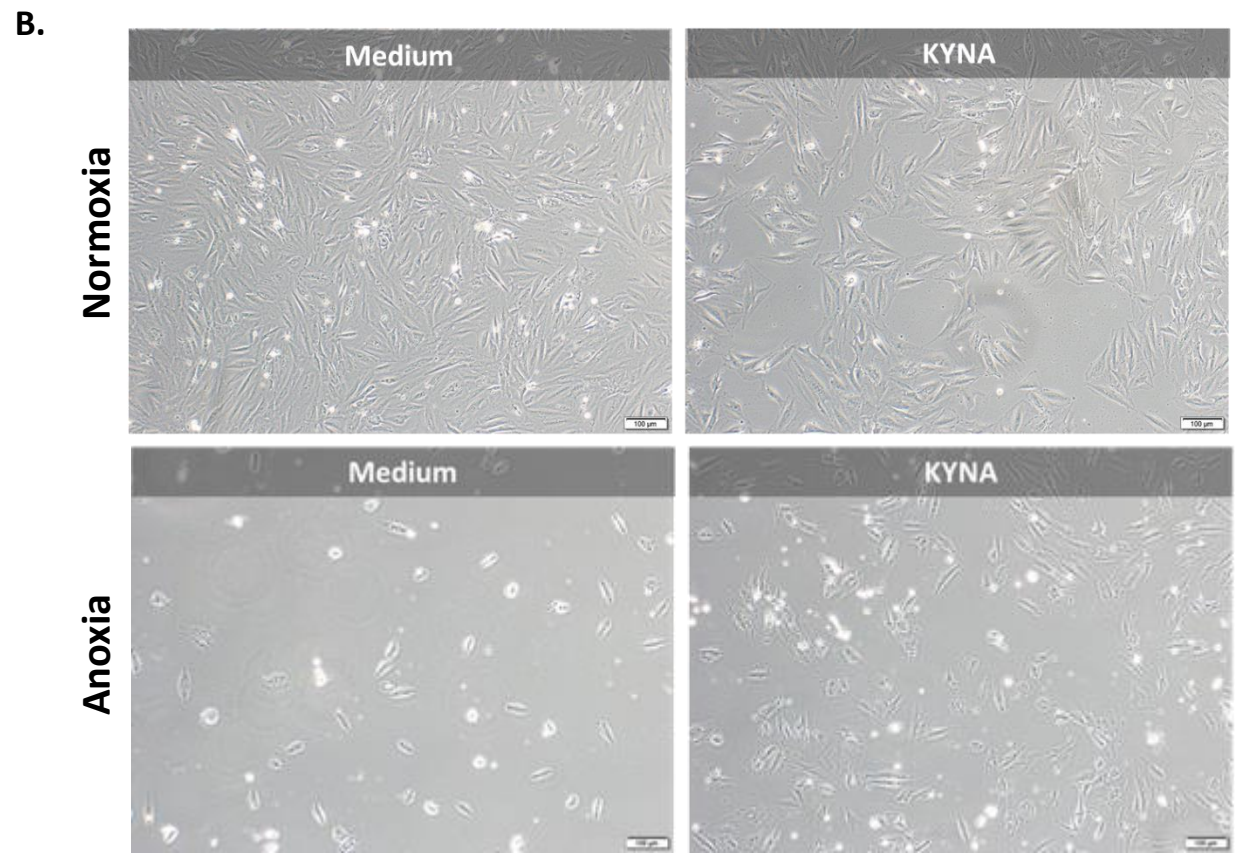

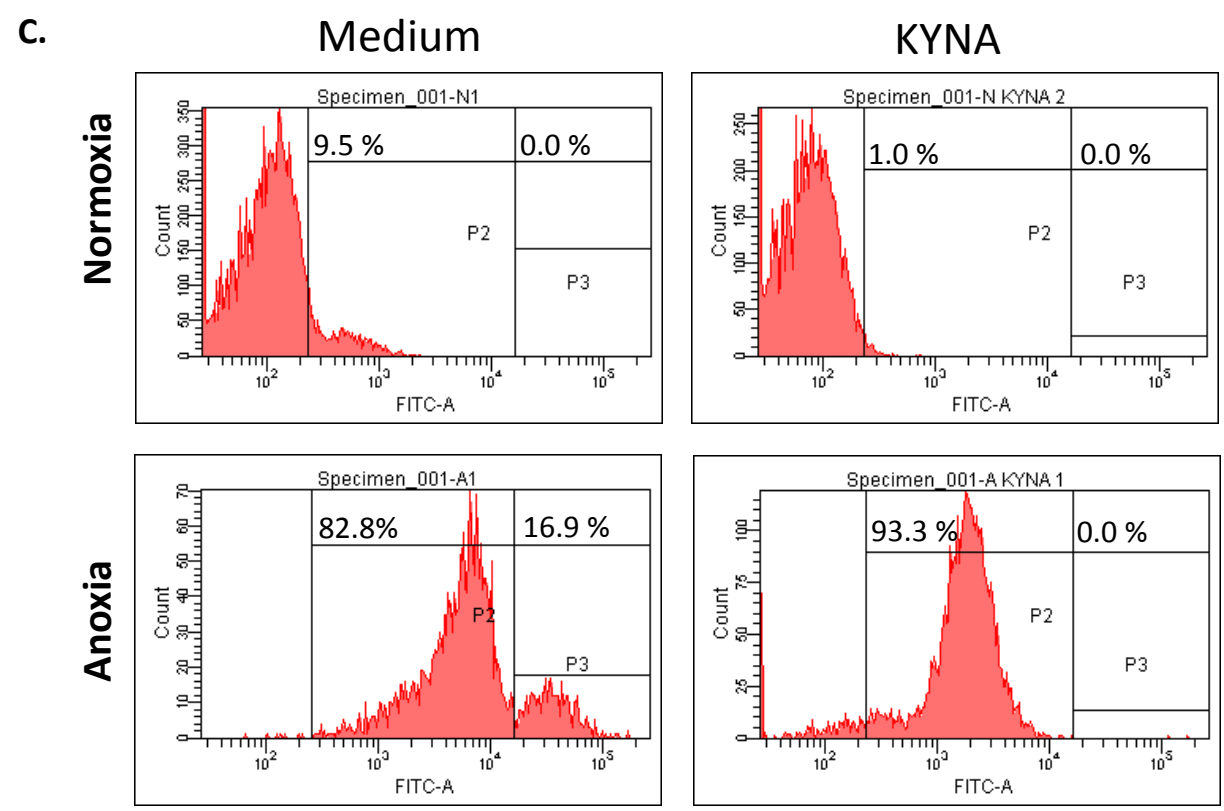

A.

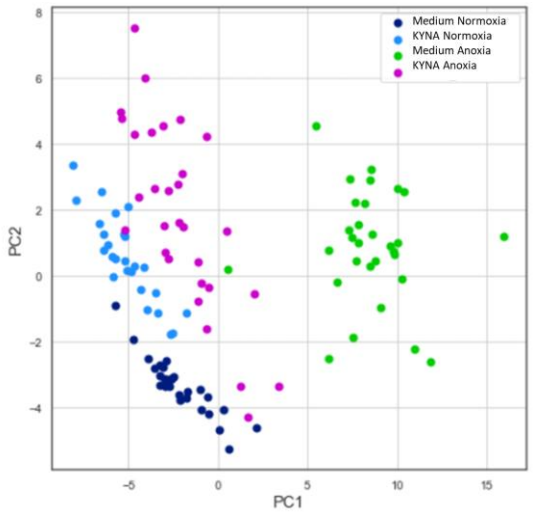
Medium Normoxia
KYNA Normoxia
Medium Anoxia
KYNA Anoxia
PC1
PC2

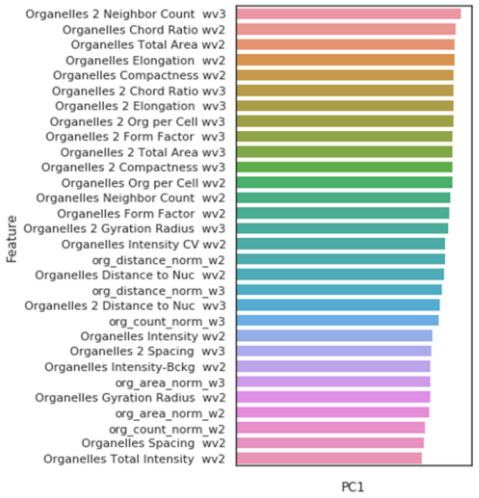
Organelles 2 Neighbor Count wv3
Organelles Chord Ratio wv2
Organelles Total Area wv2
Organelles Elongation wv2
Organelles Compactness wv2
Organelles 2 Chord Ratio wv3
Organelles 2 Elongation wv3
Organelles 2 Org per Cell wv3
Organelles 2 Form Factor wv3
Organelles 2 Total Area wv3
Organelles 2 Compactness wv3
Organelles Org per Cell wv2
Organelles Neighbor Count wv2
Organelles Form Factor wv2
Organelles 2 Gyration Radius wv3
Organelles Intensity CV wv2
org_distance_norm_w2
Organelles Distance to Nuc wv2
org_distance_norm_w3
Organelles 2 Distance to Nuc wv3
org_count_norm_w3
Organelles Intensity wv2
Organelles 2 Spacing wv3
Organelles Intensity-Bckg wv2
org_area_norm_w3
Organelles Gyration Radius wv2
org_area_norm_w2
org_count_norm_w2
Organelles Spacing wv2
Organelles Total Intensity wv2
Feature
PC1

B.

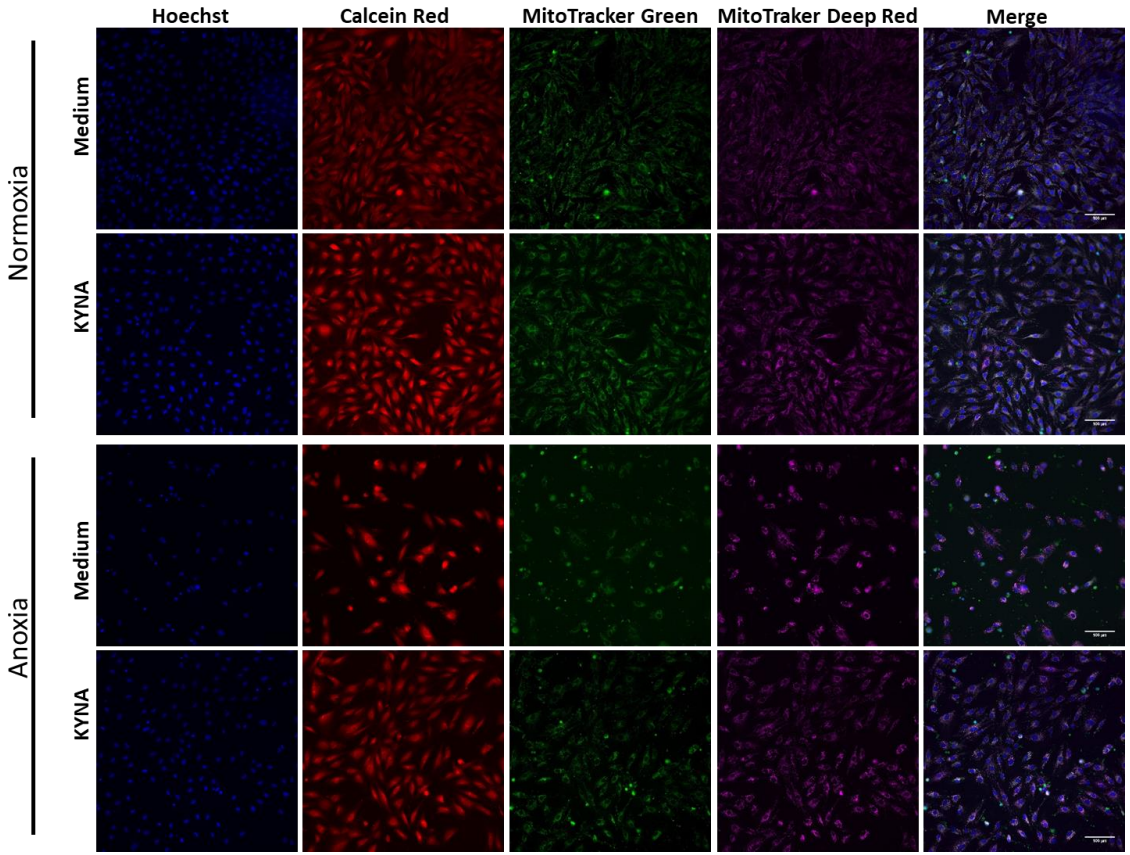
Hoechst
Calcein Red
MitoTracker Green
MitoTraker Deep Red
Merge
Normoxia
Anoxia
Medium
KYNA
Medium
KYNA

C.

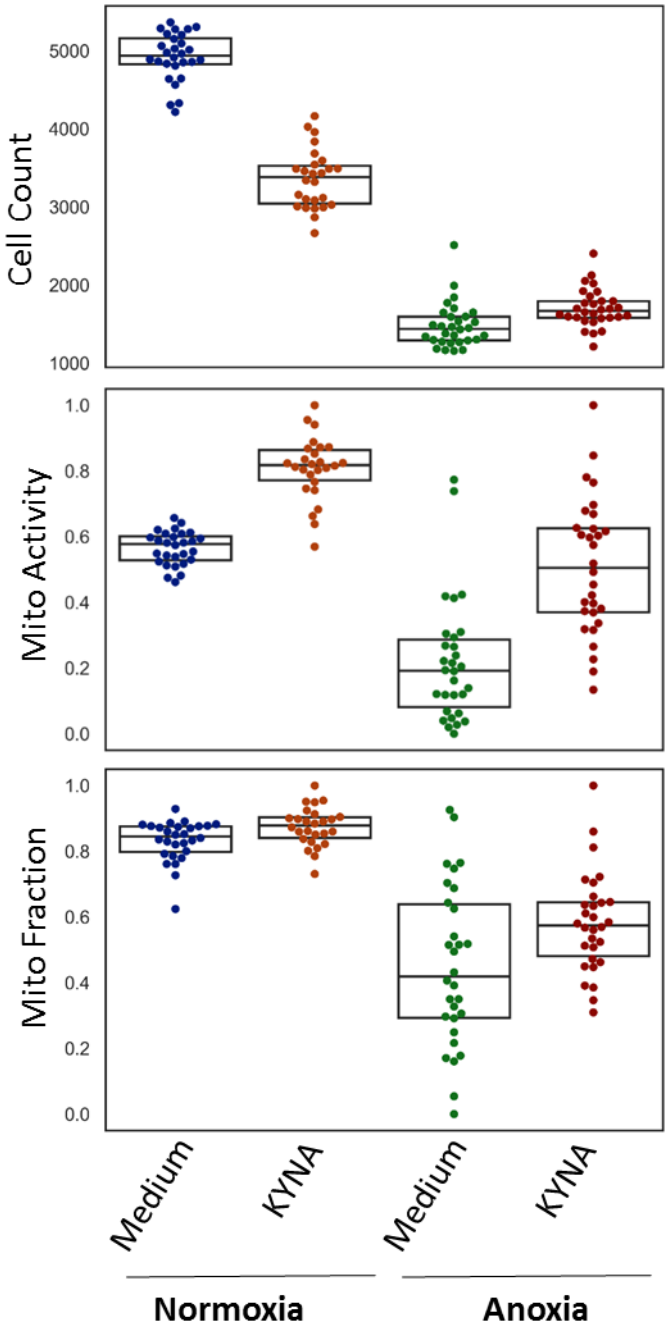
Cell Count
Mito Activity
Mito Fraction
Medium
KYNA
Medium
KYNA
Normoxia
Anoxia

A.

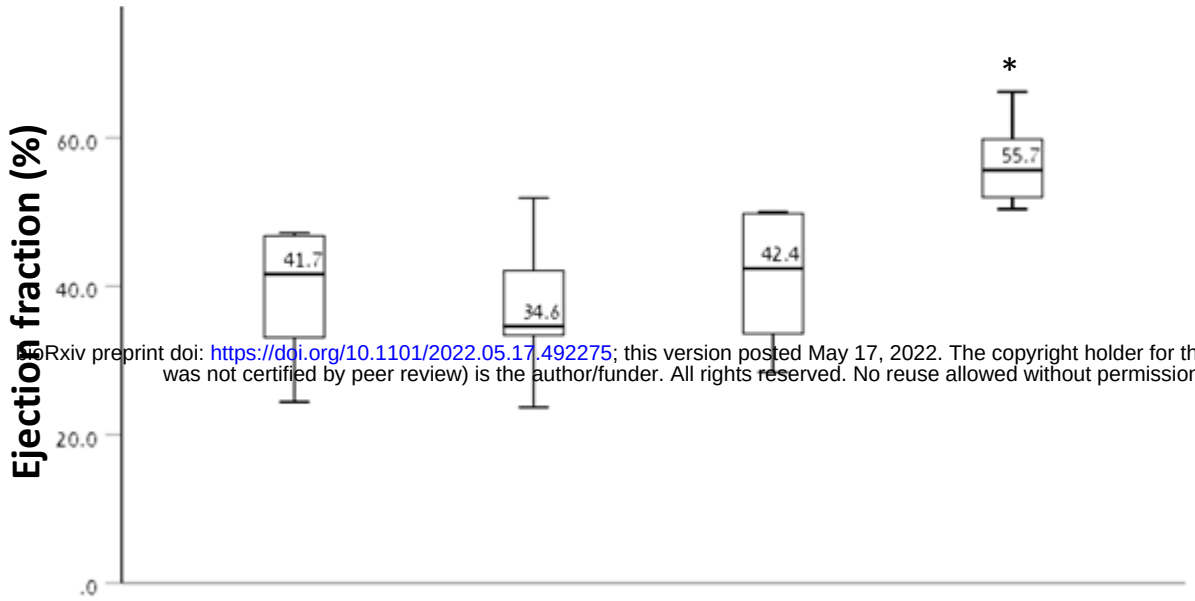

B.

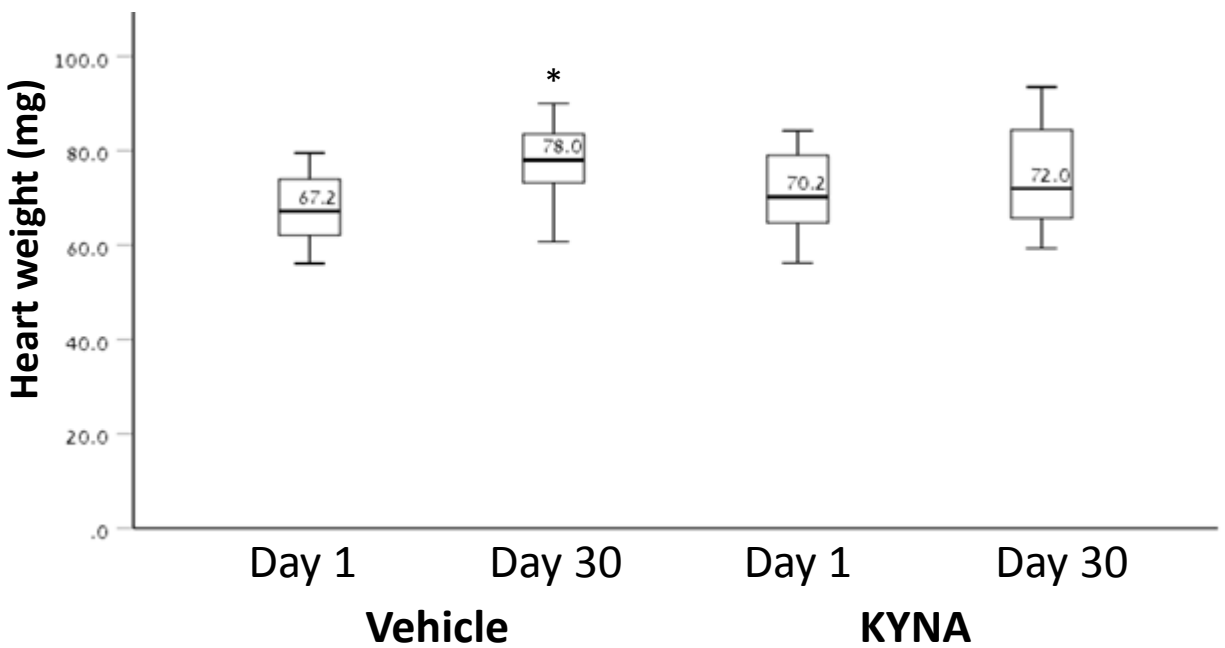

C.

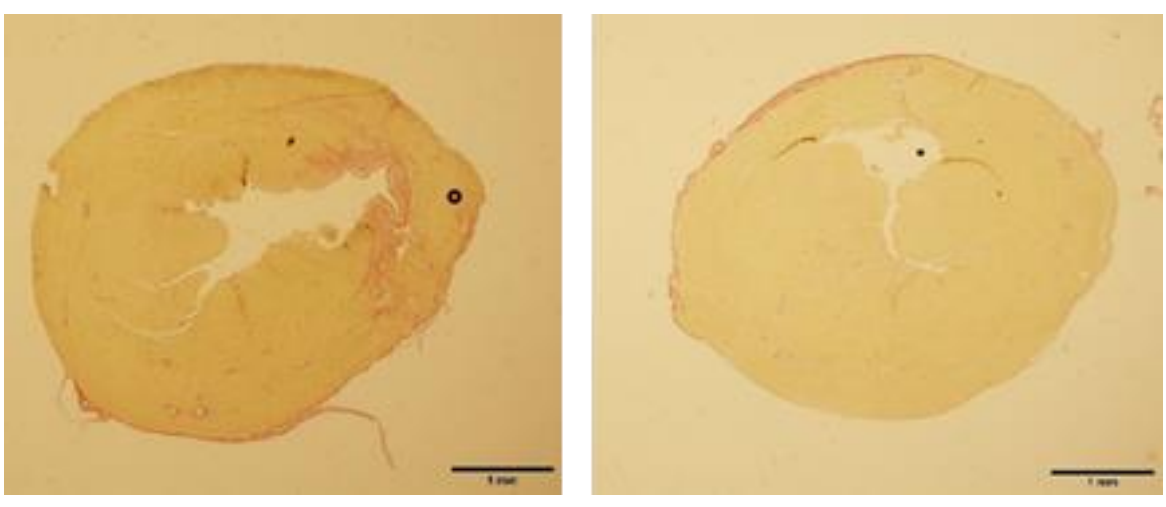

Vehicle-treated KYNA-treated